State of the Art of High-Speed MR Imaging

Felix W. Wehrli, Ph.D.
University of Pennsylvania Medical Center,
Philadelphia, Pennsylvania, USA

Introduction

Since the inception of clinical MRI at the beginning of the previous decade, the rate at which a subject can be scanned -- often denoted "patient throughput" -- has been reduced by nearly an order of magnitude. Some of the improved scan efficiency is unrelated to shortening in the actual data acquisition time and can be accounted to improvements in some of the ancillary procedures such as patient set-up, RF coil placement, scan parameter entry, prescan, and advances in digital system architecture (shortening in reconstruction times, concurrence of data acquisition and reconstruction, etc.). Scan times in excess of 5 - 10 minutes typically lead to image degradation from subject motion. Another strong motivation for shortening scan time is physiologic motion such as cardiac pulsation, respiration and peristalsis. Clearly, if the data acquisition time could be lowered below the period of physiologic motin, the effect of motion unsharpness in the image data could effectively be suppressed. Many of the new applications, such as the assessment of organ function by monitoring the passage of a bolus of contrast agent (1, 2) or the study of brain function by monitoring the passage of a bolus of contrast agent (1, 2) or the study of brain function by recording the response to stimuli (3), demand temporal resolution on the order of a second.

While many of the ideas for improved scan efficiency have been in existence for a decade or longer, they became practical only recently, owing to engineering advances such as digital transceiver electronics and high-speed gradient technology (4). A case in point is echo planar imaging (EPI), which was first conceived in 1977 (5), but which took another ten years to become practical (6, 7). Finally, increased data sampling rate typically exacts an unavoidable penalty in signal-to-noise ratio (SNR). Since the minimum tolerable SNR is usually dictated by diagnostic criteria such as lesion detectability, increases in temporal resolution will almost inevitably have to be traded against spatial resolution.

This paper briefly reviews the concepts underlying the most important classes of rapid

imaging techniques from extensions of the simple gradient echo to the family of multiline k-space scanning techniques (echo-planar, fast spin echo, GRASE), ending with non-rectilinear sampling techniques such as projection imaging, spiral scanning and BURST excitation imaging. These notes are excerpted from a recent article by the author in the Encyclopedia of Nuclear Magnetic Resonance (8). For a more detailed description of rapid imaging techniques the reader may consult the review article by Haacke and Tkach (9) and the text by Wehrli (10). Echoplanar imaging has been treated in detail by Cohen and Weisskoff (11).

K-Space Formalism

We shall, in the following use the classical k-space formalism (12-14) for describing the various imaging techniques. Though usually the realm of the physicist, we shall see that this formalism is straightforward to understand even for those not conversant in higher mathematics. An excursion into the "spatial frequency domain" ("k-space") is almost a must to enable even a qualitative description of some of the advanced imaging techniques. There is a second, and perhaps even more compelling reason: data sampling occurs in k-space. K-space, also denoted "reciprocal space", is measured in cm^{-1}, which is the reciprocal unit of length measurement. The latter, of course, is the unit used to characterize object or image space.

The signal is sampled as a function of the spatial frequency

$$k=(2\pi)^{-1}\gamma Gt \qquad (1)$$

which we can readily verified has units of reciprocal cm. From the above relationship it follows that the spatial frequency coordinate is advanced by either stepping time or varying the gradient amplitude and that the spatial frequency is proportional to the area under the gradient - time curve. The Fourier transform of this signal yields the image. Fourier's theorem states that any periodic or aperiodic function (say an object) can be thought of as constituted from a sum of sinusoids of increasing frequency (i.e. the spatial frequency). The MR signal we sample provides the weighting factors for the sines and cosines. The spatial frequency coordinate usually is a vector **k** having components k_x, k_y, k_z which are controlled by imaging gradients G_x, G_y and G_z.

In two-dimensional (2D) imaging each location of the signal map corresponds to a signal sample S (k_x, k_y). The signal near the center has the highest amplitude since it corresponds to the lowest values of k_x and k_y where spin phase coherence is greatest. Most of the signal energy is therefore stored in the low spatial frequency signals. The higher spatial frequency

signals, acquired at increased gradient strengths or increased gradient exposure time, have precessed to various extent (depending on the location along the gradient axis). The overall signal, which is the vector sum of the signals at the individual locations is thus much weaker. Nevertheless, these signals are essential in that they contain "edge information", i.e. they are necessary to provide the resolution of the image.

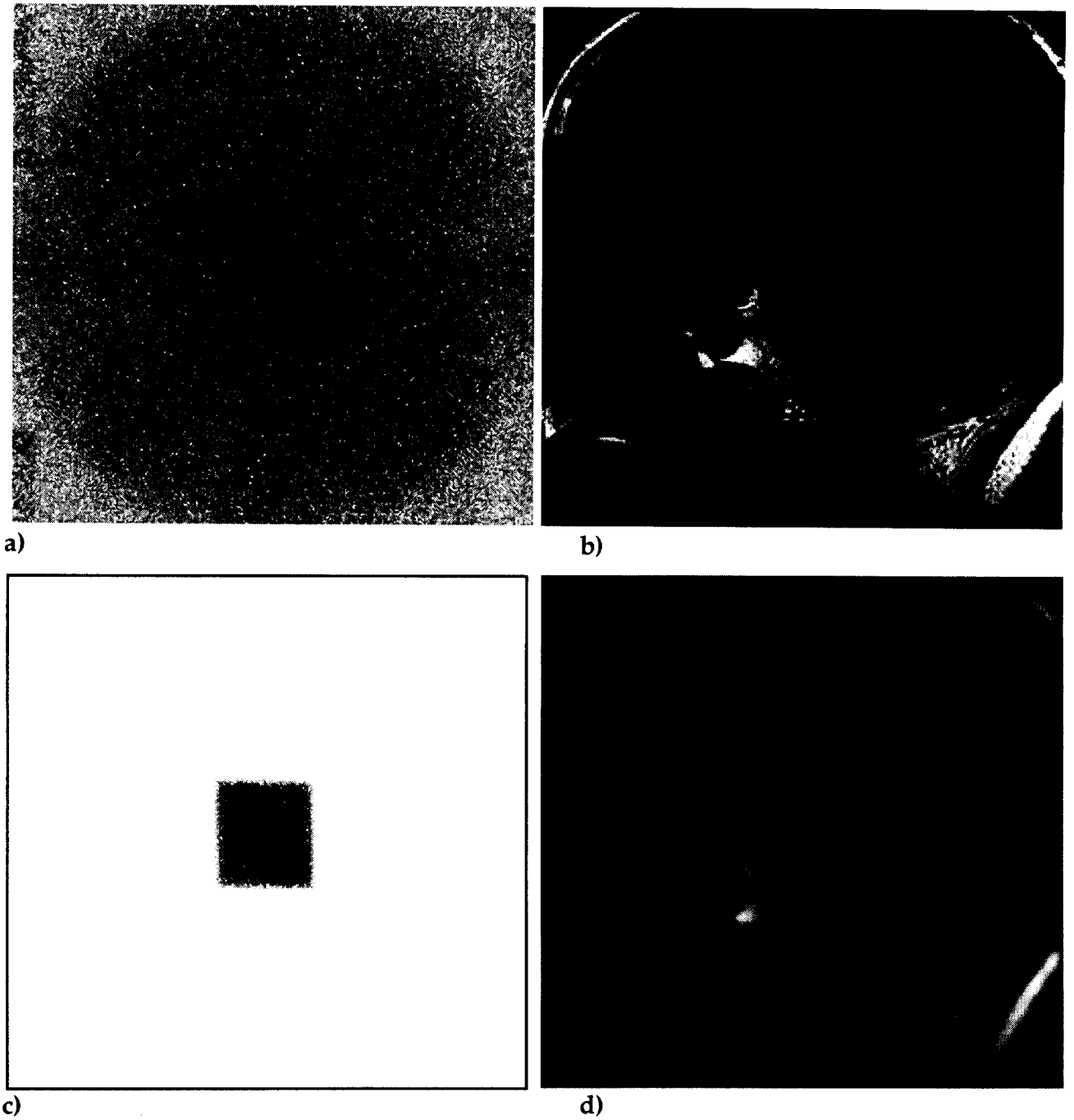

Figure 1. Effect of removal of high spatial frequency content in k-space data, causing image blurring: (a) 256x256 data samples; (b) image obtained as 2D Fourier transform of (a); (c) center 64x64 data of (a); (d) 2D Fourier transform (c).

Figure 1 shows these relationships with a brain data set. Note that removal of the high spatial frequencies has the effect of blurring the image. Whereas the larger features (e.g., corpus callosum, brain stem, etc.), are retained, small detail (e.g., pituitary gland, aqueduct, etc.) and overall edge sharpness are lost. This example nicely demonstrates the role of the high spatial frequencies in providing resolution.

Clearly, scanning only the center one sixteenth as in the case of Figure 1c) requires only a fraction of the time needed to sample the entire 256x256 data matrix. We therefore recognize that there must be a trade-off relationship between temporal and spatial resolution, i.e. we can shorten scan time at the expense of spatial resolution. We further see from the images in Figure 1 that the low spatial frequency image has higher signal-to-noise ratio (SNR).

Recalling that there is an inverse relationship between k-space and image space, it is plausible that the largest distance, i.e. the field of view (FOV) corresponds to the lowest spatial frequency. Conversely, the smallest quantum of length measurement, the pixel, is determined by the highest spatial frequency sampled. These relationship can be summarized as follows:

$$k_{max} = \frac{1}{\triangle x} \tag{2}$$

$$\triangle k = \frac{1}{FOV} \tag{3}$$

Eq [2] implies that the reciprocal of the largest spatial frequency is equal to the pixel size $\triangle x$ while Eq [3] states that the k-space sampling interval determines the FOV.

We have seen that k-space is scanned by advancing the spatial frequency coordinate which, according to Eq [1] is achieved by either changing the gradient amplitude G, or gradient duration (t). Let us now follow the spatial frequency vector, as we execute one cycle of a gradient-echo spin-warp pulse sequence (Figure 2). Since no gradients have been turned on yet at time point A the k-vector is at the center. During the time interval between A and B both gradient are negative, therefore the spatial frequency vector advances toward the edge of the third quadrant. During the readout period (A, B) only G_x is active resulting in horizontal progression of the k-vector. During the next pulse sequence cycle this process is repeated except that the phase-encoding gradient has been advanced (made less negative), which leads to parallel trajectory during readout, separated from the previous one by Dk_y. By repeating this process the entire k-space is sampled, line by line, leading to a map of data as the one shown in Figure 1a.

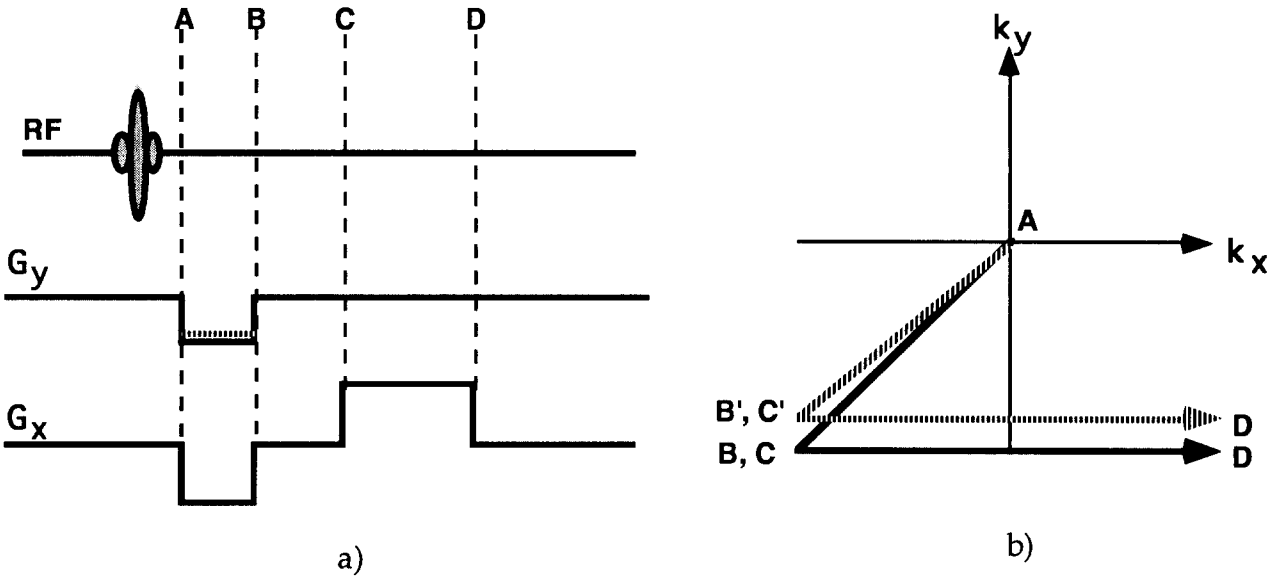

Figure 2. Gradient echo spin-warp pulse sequence (a) and K-space trajectory (b). Two pulse sequence cycles are shown. K-space coordinates K_x and K_y are determined as the signed areas under the gradient-time curves. A - D represent distinct time points.

Spin-Warp Rapid Imaging Techniques

Most of the currently used imaging techniques use rectilinear k-space sampling and as such may be regarded as descendants of Edelstein et al's spin-warp technique (15), which is illustrated in Figure 2. The spin-warp technique is an outgrowth of Fourier zeugmatography, pioneered by Kumar, Welti and Ernst (16). Since the latter is an embodiment of two-dimensional NMR spectroscopy, conceptionally all rectilinear sampling techniques may be regarded as originating from 2D NMR. By contrast, projection-reconstruction imaging (17-19) or imaging with nonperiodic time-varying gradients (20) such as spiral scanning (21, 22) are not rectilinear sampling techniques since the k-space path is non-Cartesian.

Common to all rectilinear k-space sampling techniques are two distinct phases of spatial encoding, a first period during which a gradient G_y is applied whose time integral determines k_y and during which no sampling occurs, followed by a second period during which a gradient G_x is applied while the free precession signal is sampled, resulting in a line k_x. The former is typically called "phase encoding", the latter "frequency encoding". In this manner a 2D k-space grid is sampled by incrementally stepping the amplitude of the phase-encoding gradient. The concept

can be extended to a third dimensional. In both back-projection and spiral scanning two or all three spatial encoding gradient are simultaneously active while data are sampled.

Various Embodiments of Spin-Warp Imaging

Characteristic to the spin-warp technique is that only one line of k-space is typically scanned upon creating transverse magnetization, and the process repeated several times, each cycle affording an additional line. Longitudinal magnetization builds up in a recurrent fashion between cycles of period TR (also called "pulse repetition time"). The data acquisition time thus scales with TR and the number of pulse sequence cycles, the latter being a function of the number of spatial encoding steps or k-space samples.

At typical sampling rates the sampling time for frequency encoding is on the order of 5 - 10 milliseconds. It is thus much shorter than the pulse repetition time, which typically is on the order of hundreds of milliseconds or longer, and thus does not significantly affect scan time. It will, however, become critical in high-speed gradient-echo imaging (23, 24) and EPI and its derivatives (11).

Scan time scales with the number of phase encodings (N_y in 2D, and N_y and N_z in 3D spin-warp imaging) and thus a reduction in the number of phase encoding samples entails a concomitant reduction in scan time. However, this can be achieved in two different ways; either by lowering k_{max} or decreasing sampling density ($1/\triangle k$). The former lowers resolution, the latter leads to reduced field of view while preserving resolution (cf. eqs. (4) and (5)). Thus, the term "matrix size" is ambiguous, though in common parlance a change in matrix implicitly implies fixed field of view.

Slice Multiplexing and Conjugate Synthesis

In most embodiments of 2D spin-warp imaging the period comprising slice selection, phase-encoding and frequency-encoding accounts for only a fraction of the TR interval. Therefore minimizing the dead time by shortening the pulse recycle time seems to be a straightforward means of optimizing scan time. However, TR is typically dictated by contrast requirements. Shortening of TR leads to progressive saturation. A solution to this problem, first mentioned by Brunner and Ernst (25) was given by Crooks et al. (26) who introduced what is commonly denoted 2D multi-slice imaging. By making the RF pulses slice-selective, the spins in the slice of interest only are stimulated. Adjacent slices are then excited in sequence without

perturbing the steady state. The gain in efficiency achieved in this manner depends on TR, the echo time TE, and the time required for applying the spatial encoding gradients and typically ranges from about 10 to 50. The second important innovation was the incorporation of Carr-Purcell echoes into spin-warp imaging. In this manner images with different contrast can be derived from a single acquisition. It is obvious, that adding echoes reduces the number of slices that can be interrogated in a given TR period. Both, 2D multi-slice and multi-echo spin-warp imaging, perhaps appearing trivial in hindsight are, in historic perspective, among the most significant milestones in the quest for imaging efficiency.

A salient property of k-space with implications on imaging speed is its conjugate symmetry. Since **k** and **-k** are identical, it suffices in principle, to acquire only half of k-space. In reality, however, the conjugate symmetry is often not perfect. Causes for deviations are phase shifts from magnetic field inhomogeneity and motion which require appropriate correction of the raw data before Fourier reconstruction (27).

As already pointed out, sampling in k_y, k_z direction is much slower than sampling in k_x direction. Therefore, by exploiting the redundancy in phase encoding lines, scan time is halved. Halving imaging time by conjugation was described by Margosian et al. (28) and by Feinberg et al. (29) and MacFall et al. (27). Because the phase correction requires sampling of a small number of data lines on the conjugate half, the time savings is usually somewhat less than 50%.

Variable Flip Angle Imaging

In their seminal work on pulse Fourier transform spectroscopy Ernst and Anderson (30) showed that for a train of equidistant RF pulses the extent of saturation can be controlled by adjusting the RF pulse flip angle α and further that the signal peaks for the condition

$$\alpha_{opt} = \cos^{-1}(e^{-TR/T1}) \qquad (4)$$

In Eq (4) α_{opt} is optimum pulse flip angle (also denoted "Ernst angle") which is valid provided that TR>>T2 holds. It is readily recognized that flip angles $\alpha < 90^\circ$ are not compatible with the simple Hahn or Carr-Purcell imaging pulse sequence since inversion of the residual longitudinal magnetization by the subsequent phase reversal pulse would lead to a steady state of very low magnetization. Haase et al. (30) modified the original spin-warp technique in which a gradient echo is sampled and showed that in this manner TR could be reduced at least 10-fold relative to corresponding spin-echo implementations, which may have prompted the authors to the

acronym "FLASH" (fast low angle shot). Other solutions to the problem involve the idea to restore the longitudinal magnetization with a second 180° pulse (31). An alternative solution is to select a flip angle so that 90° $< \alpha <$ 180° , followed by the usual phase-reversal 180° pulse (32, 33). In contrast to FLASH the latter techniques provide true spin-echo images in which the signal is attenuated as $\exp(-TE/T_2)$ rather $\exp(-TE/T_2^*)$ as in FLASH. This application is important for imaging tissues and biomaterials which are intrinsically inhomogeneous due to variations in magnetic susceptibility. Partial flip-angle spin-echo methods have therefore been successful for obtaining ultra high-resolution images of the trabecular microstructure (31) and, more recently, of the skin (32) in vivo.

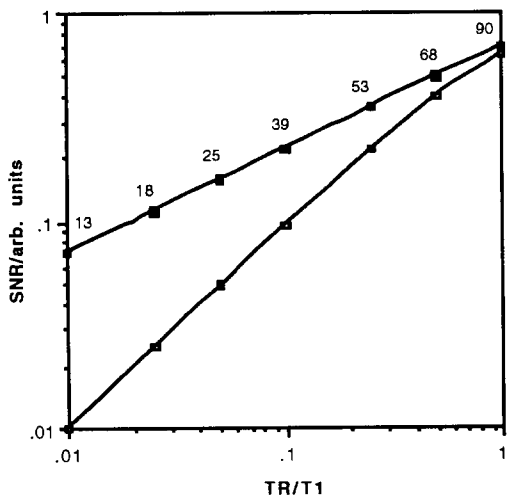

Figure 3. Signal amplitude as a function of TR/T_1 for repetitive pulses after attaining steady state: $\alpha = \alpha_{opt}$ (upper curve, with optimum flip angle indicated), and α=90° (lower curve), assuming negligible residual transverse magnetization.

The FLASH signal intensity at the optimal flip angle can be shown to be proportional to tan (α/2). In Figure 3 the relative SNR is plotted as a function of TR/T_1 for α=90° and $\alpha = \alpha_E$. In either case shortened data acquisition time exacts a SNR penalty which, however, is less severe if the flip angle is optimized. At typical imaging field strengths (1±0.5T) mammalian tissue T1 relaxation times span a range of about one order of magnitude (from ca. 0.3 s for fat to about 3 - 4 s for extracellular fluids). Hence a compromise setting will have to be chosen for α. As the flip angle is gradually increased, gradual saturation occurs and thus progression from proton density to T1-weighting. Low flip angles emphasize structures with long T_1 such as cerebrospinal fluid in the ventricles.

High-Speed Gradient-Echo Techniques

Combination of increased sampling frequency bandwidth and fractional echo sampling with partial Fourier processing, reduction in the number of frequency-encoding samples and other strategies such as truncated RF pulses, permit shortening of pulse repetition times to 5 ms or less (23, 24, 33). Clearly, these methods need to be assessed in terms of the benefits and trade-offs they entail. Besides SNR, contrast is perhaps the single most important criterion for clinical utility. The typically unsatisfactory contrast inherent to high-speed steady-state techniques can be enhanced by means of magnetization preparation (23, 34-36). The underlying idea is to create a non-equilibrium situation by preceding the train of low-angle RF pulses by an inversion pulse for T1-weighted contrast (23, 34, 35) or driven-equilibrium pulses to achieve T2-weighted contrast Mugler, 1991 #701]. Since in this case the magnetization evolves during scanning of k-space, effectively filtering the data in a manner determined by the spin dynamics, the usual sequential scanning from $-k_{max}$ to $+k_{max}$ is not optimal. Remembering that the signal components pertaining to k=0 contribute most to contrast, it is necessary to acquire these data at the desired time point during magnetization evolution (for example when the signal from a particular tissue is nulled. These requirements can, for example be reconciled with a k-space ordering scheme which has been denoted "centric phase encoding" (34), in which data collection starts at k-space center and proceeding outward.

Finally, we can trade the increased efficiency of high-speed gradient-echo imaging can be exploited for generating very ultra high-resolution images, as first demonstrated by Foo et al. (33). Similar technology was recently used in the author's laboratory for obtaining microscopic images of the human skin in vivo at voxel sizes as small as 20x80x800 μm^3 (32).

A comprehensive review of short-TR imaging techniques has recently been published (9)

Cardiac Gated Techniques

Except when the entire k-space can be covered in a small fraction of the cardiac cycle, such as in EPI imaging, data acquisition in cardiac imaging needs to be synchronized to the cardiac cycle. Therefore, the minimum scan time in 2D spin warp imaging of the heart appears to be given as Ny · Tc with Ny and Tc being the number of phase-encoding samples and cardiac period, respectively. The inherent speed of the gradient echo then can be exploited to subdivide the cardiac period by collecting data at multiple cardiac phases resulting in a series of temporally resolved images which can be played back in a movie loop, a technique which has been called "

cardiac cine" imaging (37, 38). The minimum scan time can be considerably shortened (albeit at some cost in temporal resolution) if, instead of a single line ky, multiple lines are scanned per cardiac phase. This modification, also termed "segmented k-space" acquisition (39) permits shortening of the data acquisition time in cardiac cine imaging to 16-24 heart beats (39, 40) which is within the range of a breath-hold period, therefore considerably improving cardiac image quality.

Multi-Line Scanning Techniques

All previously discussed embodiments of spin-warp imaging have in common that within one pulse sequence cycle a single data line is sampled. Additional echoes are merely a replication of the procedure affording images of increasing T2 weighting. An inherently more efficient approach makes use of the idea to exploit a plurality of echoes in such a manner that each echo affords a separate k_y line.

Echo Planar Imaging

In 1977 Mansfield first proposed what he termed "echo planar imaging" (EPI) in which the entire 2D encoding process could be completed during a single FID. The fundamental principle underlying the technique is to oscillate the read gradient G_x in the presence of a constant gradient Gy (41). It is readily seen that in this manner half of k-space is traversed in a zig-zag trajectory. The difficulties in reconstructing images from only half the data and non-orthogonal sampling grids were remedied with the introduction of pre-encoding gradients and discontinuous phase-encoding (6, 7, 42, 43). In this manner, Pykett and Rzedzian obtained entire images from 64x128 data samples in as little as 50 ms at 2 T field strength (6, 7). For an overview of the subject the reader is referred to the review by Cohen and Weisskoff (6).

In Pykett and Rzedzian's approach (6, 7), short phase-encoding gradients prior to each readout lead to a stepwise progression across k_y. Further, pre-encoding gradients are applied so that k_y is scanned from $-k_{y,max}$ to $+k_{y,max}$, as shown in Fig. 4. We can now, as shown earlier, construct the k-space trajectory from the gradient areas traversed at the various time points, labeled t_A through t_F (Fig. 4b). At time point t_A, before turning on any of the spatial encoding gradients, $k_x=k_y=0$ (center of k-space). After simultaneous application of the two pre-encoding gradients, k_x, k_y advance to point B, the largest positive value of k. The subsequent 180° phase-reversal pulse leads to the corresponding conjugate location -k, i.e. the most negative k-value (point C). During the next-following time interval (t_C t_D), during which only the positive read gradient is active, we sweep across k_x (with k_y constant) to end up at point D. Note that

k_x=0 corresponds to the center of the gradient echo which is attained when the area of the pre-encoding lobe of the frequency-encoding gradient is exactly equal to the area under the frequency-encoding gradient. Another important feature of this pulse sequence is that the center of k-space is traversed at the time of the Hahn spin echo. The k-trajectory in Fig. 4b scans k-space "bottom - up". It is readily seen that reversing the polarity of the y gradients would result in a top - down trajectory. The two approaches are, of course, equivalent.

Perhaps the greatest technical challenge is to administer the gradient train sufficiently fast since the signal persists only for a time on the order of T_2^*. Thus the entire N_p x N_f samples have to be taken during a period comparable to T_2^*. It therefore becomes evidence that an echo planar imaging system has to operate a much higher sampling frequency than its conventional imaging counterpart. Further, the gradients need to be switched very rapidly, which requires short rise times. The phase encoding "blip" has to be applied very rapidly as well to minimize total readout time. Since the higher spatial-frequency signals are weighted as $e^{-TE(k_Y)/T2^*}$, the technique is subjected to similar limitations as the fast spin-echo (FSE) technique, discussed below, i.e. blurring in phase-encoding direction due to relative de-emphasis of high spatial frequency components may occur. In practice, however, this constraint is less severe since the resolution targeted with EPI is usually lower than in FSE, with emphasis being on temporal resolution.

With current technology (>20 mT/m gradient amplitude and ~200 T/ms slew rate), it is possible to acquire 128x128 echo planar images in less than 100 ms scan time. The insensitivity to motion will be exemplified with images obtained while the subject was deliberately performing a left-right tilting motion of the head. While the motion resulted in gross overall displacements of the head, no effects of motion unsharpness or artifacts are seen. In neuro imaging EPI will undoubtedly have applications for examining uncooperative patients and children who have to be sedated with conventional imaging techniques.

When generating a train of gradient echoes under a spin-echo envelope, in which case the zero spatial frequency signals are collected at the time of the Hahn echo, the images are inherently T2-weighted. In functional imaging, which makes use of the BOLD contrast phenomenon, T_2^* weighting is required. Under these constraints it is desirable to acquire the low spatial frequencies k_y data for a gradient echoes with 30-50 ms echo time. For this purpose a gradient echo-planar technique is better suited. It is analogous to the pulse sequence of Fig. 4 except that the gradient echo train begins immediately following a reduced flip-angle RF pulse.

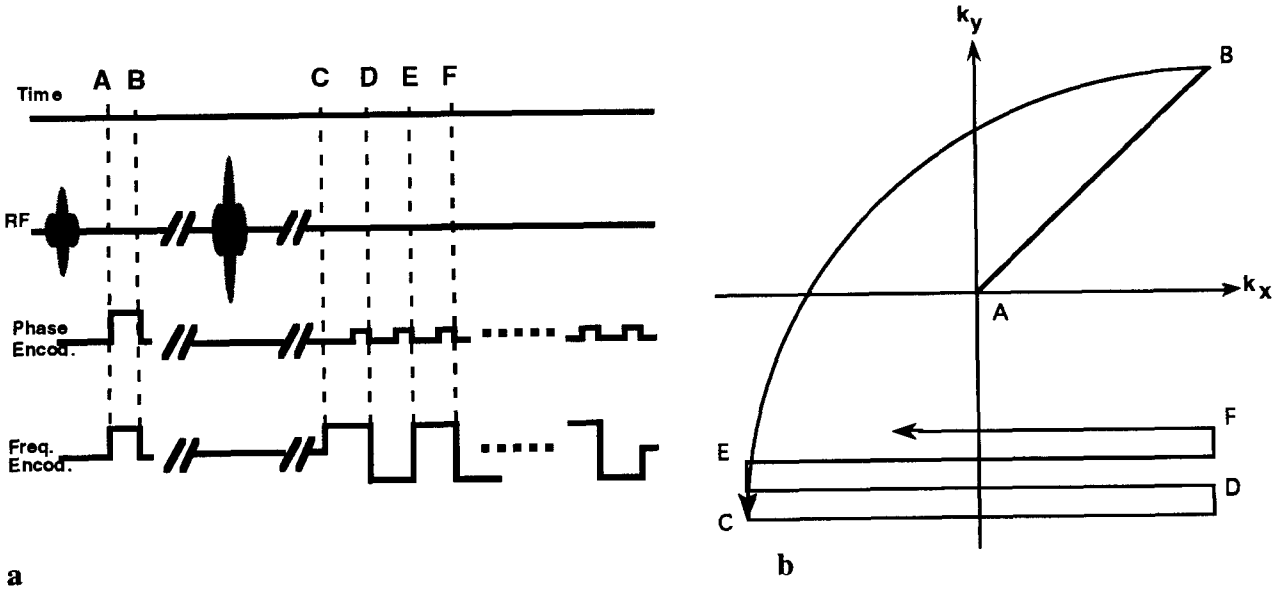

Figure 4. a) Spin-echo EPI pulse sequence: A spin echo is produced so that k_y=0 is traversed when spins are completely rephased, i.e. at echo time TE. Pre-encoding gradients ensure that both halves of k_y-space are scanned symmetrically. The time points t_A - t_F correspond to locations A - F in the K-space trajectory (Fig. b). Note that the effect of the 180° pulse is to bring $+k_{x,y,max}$ to its conjugate $-k_{x,y,max}$. Each phase-encoding 'blip' advances k_y by increment $\triangle k_y$. For simplicity, slice-selection gradients are not shown in (a).

An interesting corollary of single-shot EPI is that the pulse repetition time loses its meaning since the data are collected in single sequence cycle. However, concatenation of individual acquisitions for the purpose of generating movies, for example, underlines the same restrictions as the conventional FLASH method, demanding adjustment of the RF flip angle to control saturation. Chapman et al. (44) and Cohen and Weisskoff (44) showed cardiac movies obtained by acquiring a complete set of images with in a single heart beat. Unlike gated techniques where each image data set, or fraction thereof, is collected during consecutive heart beats, the method is insensitive to variations in heart rate.

In contrast to the high-speed FLASH-type methods, however, echoplanar imaging puts fat more stringent demands on instrumentation, in particular to amplitudes and slew rates of the gradients, which explains its currently limited diffusion. Some of these conditions are relaxed if only a fraction of k-space is scanned from a single echo train. For many clinical applications so-called interleaved EPI (45, 46) is therefore better suited. Whereas this variant of EPI is no

longer 'real time', the quality of the images is far superior since the readout times are considerably shorter and thus phase errors from magnetic field inhomogeneity less severe. Scanning k_y-space in eight interleaves, for example, permits scanning of an entire volume in a multi-slice fashion, takes only eight TR periods and thus affords high-resolution images of very good quality in less than a minutes scan time.

Finally, one wonders what SNR penalty this extraordinary scan speed exacts. At a given resolution three parameters contribute to SNR: (i) sampling time (SNR $\sim\sqrt{}$ts), (ii) transverse relaxation losses (SNR$\sim e^{-TE/T2}$), and (iii) the fraction of magnetization available for signal creation determined by saturation (SNR$\sim$f(TR, T1,. α)). The following comparison may be instructive. Suppose a typical tissue such as neural white matter is scanned at 1.5 T field strength (T1$\sim$ 700ms, T2$\sim$75 ms). Then let us consider a high-speed gradient-echo acquisition with 128 phase encodings and 2ms readout time, TR=5 ms, TE$\sim$0, operated at the optimum flip angle, which is 6.8° , and compare it to a single-shot EPI with 50 ms total sampling time, performed such that k_y=0 is sampled at TE=30 ms. The results are summarized in Table 1. They imply a net advantage of about a factor of 5 in favor of EPI., defeating the common notion that shortened scan time inevitably exacts a SNR penalty !

Similar arguments in favor of EPI have been put forward in ref. (44). Such a comparison, however, does not withstand more rigorous scrutiny. Suppose we were to repeat the EPI scan every 640 ms, i.e. the equivalent of the FLASH data acquisition time. This would mean that the longitudinal magnetization has only incompletely recovered, therefore requiring operation at the Ernst angle, which is 65° . Doing so reduces the transverse magnetization following the RF pulse to 0.64 (from eq. (12a)), thus lowering the relative SNR advantage of EPI to (a still substantial) factor of 3.

Table 1.

Comparison of SNR in single-shot EPI and high-speed FLASH. For assumptions see text.

	EPI	FLASH	SNR_{EPI}/SNR_{FLASH}
Sampling Time (ms)	50	256	0.44
Magnetization	1	0.06	16.7
exp(-TE/T2)	0.67	1	0.67
Net gain			4.9

RARE (Fast Spin Echo)

In 1986 Henning (47) introduced the spin-echo counterpart of EPI, initiating a development with significant impact on clinical efficiency. Surprisingly, this work did initially not elicit broad interest. The perception that the images emphasized structures with long T_2, thereby producing significantly T_2-weighted images, prompted Henning to dub his technique "RARE", short for rapid acquisition with relaxation enhancement. While obviously highly efficient, the extreme T_2 weighting appeared to limit the method to specialized applications such as imaging of cerebrospinal fluid. More recent embodiments of the technique are typically referred to as fast spin echo (FSE) or 'turbo spin echo' (TSE).

Besides scan time reduction by up to an order of magnitude, the current widespread clinical use of the method owes its popularity to their spin echo nature, i.e. being insensitive to magnetic field inhomogeneities. Equally important, however, is the almost unlimited latitude in image contrast RARE provides if implemented in a hybrid mode with only a fraction of k-space covered per echo train. It is interesting that the possibilities for contrast manipulation of the RARE sequence was already recognized by Henning in his 1986 paper (47). By appropriately k-space weighting the echoes Melki et al. (48) showed that virtually any arbitrary contrast is possible. For this purpose they devised an algorithm for phase-encoding ordering while minimizing adverse effects from discontinuous sampling of k_y space. For example, assigning early echoes to low spatial frequencies, de-emphasizes T2 weighting. The convolution of the data with the relaxation function, of course, may result in point spread function blurring since high-k signals are attenuated (49, 50).

Since each of the n echoes generates n lines k_y., the minimum data acquisition time is lowered n-fold. Nevertheless, when assessing the method's efficiency in terms of scan time per image, one has to consider that the prolonged echo train reduces the number of slice locations which can be interleaved during the dead time following data collection. For example, at an echo train length of 250 ms consisting of 16 echoes, a TR=3 s acquisition provides for fewer than 12 slice locations which can be interleaved during the dead time following data collection. For example, at an echo train length rather than ~30 as for a conventional dual-echo scan with a second echo time of 100 ms. Henning showed that the per-unit-time SNR can be up to a factor of 100 higher in single-shot RARE, which again emphasizes what we have seen for EPI, i.e. that increased scan speed does not inevitably penalize SNR. Therefore, the greatly improved efficiency can be traded for improved resolution (by a factor of four in linear resolution) without adversely affecting SNR when compared to single-line spin-echo imaging. Further, it enables 3D

imaging with all its benefits such as retrospective data rearrangement with image display in secondary planes, which was hitherto impractical in the spin-echo imaging because of excessive scan time (51). Finally, it has also been shown that RARE and EPI principles can be combined in such as manner that gradient echoes are interleaved into a spin-echo train and thus the efficiency further augmented. This technique has been dubbed GRASE (gradient and spin echo) (52).

Like the EPI RARE can be operated in s single-shot mode (53). At high magnetic field, however, the large temporal density of 180° pulses would lead to prohibitive RF power deposition, which requires the sequence to be run by lowering the flip angle of the refocusing pulses (53). This constraint poses additional problems, the formation of stimulated echoes and the concomitant amplitude modulation of the echoes due to varying contributions form these echoes. This problem has recently been solved by Alsop (54) who devised a scheme of varying flip angle which ensures a smooth and rapid approach to steady state and a high steady amplitude of the signal. Appropriate assignment of the spatial frequencies to the echoes permits contrast manipulation in a manner analogous to the fast spin echo (48). In distinction to the conventional fast spin echo using 180° that is considerably longer, which is a consequence of the stimulated echoes which evolve with a time constant T_1 (which is typically longer than T_2). While only slightly longer scan times than single-shot EPI, the single-shot RARE images are free from susceptibility artifacts (Figure 5).

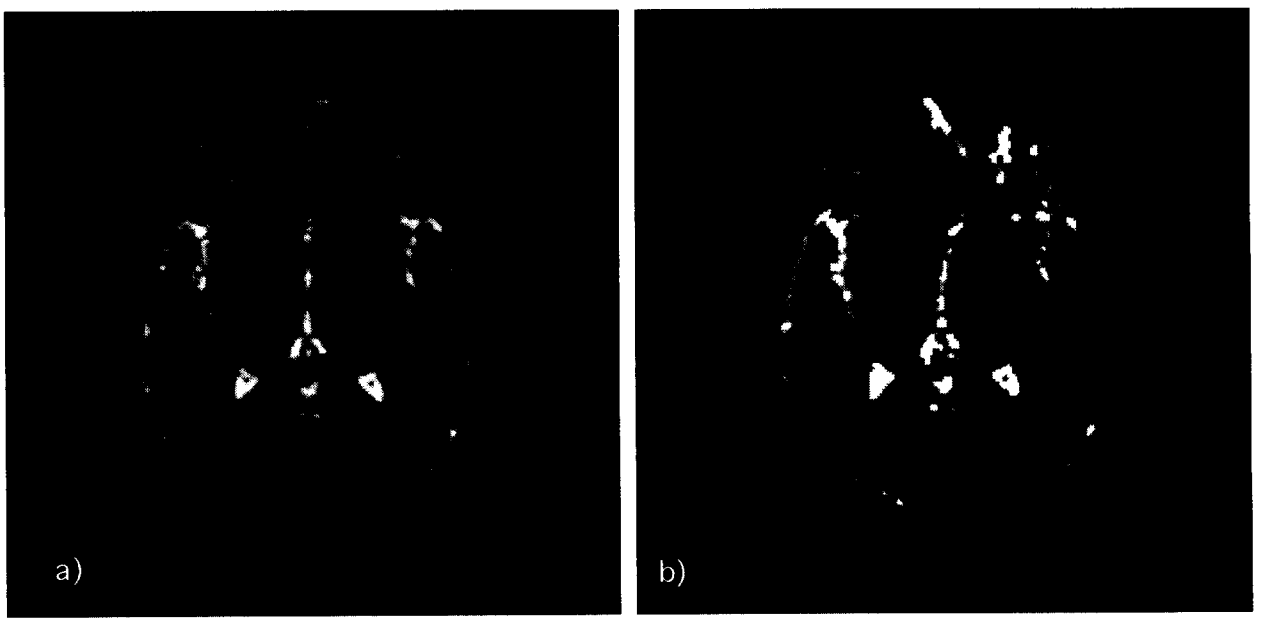

Figure 5. Comparison of single shot partial flip-angle RARE (a) and single-shot EPI images (b). Note the absence of susceptibility artifacts in the RARE images. Total acquisition times were 400 ms and 100 ms, respectively. (Courtesy D.C. Alsop, Department of Radiology, University of Pennsylvania)

Other Methods of Scanning k-Space

An alternative k-space scanning technique which, like EPI uses oscillating gradients, is spiral scanning. As implied by the term, the k-space trajectory in this case is a spiral originating at k-space center. Ahn et al. (21), who published the first spiral-scan images, used a back-projection algorithm for reconstruction. Most of the more recent work is based on constant-velocity interleaved k-space spirals (as opposed to constant angular frequency), an embodiment which is credited to Macovski's laboratory (22). This scanning mode has the advantage that k-space is covered more uniformly and that the amplitude of the oscillating gradients is constant. Compared to EPI the gradient amplitude and slew rate requirements are less demanding and the technique has been found to tolerant to flow-related dephasing, an observation which was accounted to the low gradient moments near k-space center and the periodic simultaneous return to zero of all moments.

Spiral scans require different reconstruction algorithms. Fourier transformation along the radial coordinate affords a series of projections from which the image is obtained by filtered back projection. Alternatively, the data can be rearranged into a rectilinear grid by interpolation, thus allowing Fourier reconstruction (22).

In summary, during the past two decades since its inception, MRI has revealed a wide spectrum of technical approaches for covering data space. Scan speeds a continuum ranging from milliseconds to minutes with trade-offs between temporal resolution, SNR and spatial resolution. The rate at which k-space can be scanned is significantly determined by the imager's hardware, in particular the achievable amplitudes of the spatial encoding gradients and their switching rates, and the receiver's bandwidth. Besides intrinsic SNR, the ultimate scan speed may be limited by adverse bioeffects. notably peripheral nerve stimulation caused at increased dB/dt of the switched gradients (55).

References

1. P. S. Tofts and A. G. Kermode. Measurement of the blood-brain barrier permeability and leakage space using dynamic MR imaging. 1. Fundamental concepts. Magn Reson Medicine 17, 357 (1991).
2. P. S. Tofts, B. Berkowitz, and M. D. Schnall. Quantitative analysis of dynamic Gd-DTPA enhancement in breast tumors using a permeability model. Magn Reson Medicine 33, 564 (1995).
3. K. K. Kwong, J. W. Belliveau, D. A. Chesler, I. Goldberg, R. Weisskoff, B. Poncelet, D. Kennedy, B. Hoppel, M. Cohen, R. Turner, H. Cheng, T. Brady, and B. Rosen. Dynamic magnetic resonance imaging of human brain activity during primary sensory stimulation. Proc Natl Acad Sci 89, 5675 (1992).
4. D. Weber, in General Electric Publication #3187. 1993),
5. P. Mansfield. Multiplanar image formation using NMR spin echoes. J Phys C 10, L55 (1997).
6. I. L. Pykett and R. R. Rzedzian. Instant images of the body by magnetic resonance. Magn Res Medicine 5, 563 (1987).
7. R. R. Rzedzian and I. L. Pykett. Instant images of the human heart using a new, whole-body MR imaging system. Am J Roentgenol 149, 245 (1987).
8. F. W. Wehrli. in Magnetic Resonance Imaging I. R. Young, Eds. (John Wiley & Sons, Chichester, England. 1995), vol. 8, pp. 5020.
9. E. M. Haacke, P. A. Wielopolski, and J. A. Tkach. A comprehensive technical review of short TR fast magnetic resonance imaging. Rev Magn Res Medicine 3, 53 (1991).
10. F. W. Wehrli. Fast-Scan Magnetic Resonance: Principles and Applications (Raven Press, New York, 1991).
11. M. S. Cohen. High-speed imaging: from fast to instant. Magn Res Imaging 8 (Suppl 1). 177 (1990).
12. P. Mansfield and P. K. Grannell. NMR 'diffraction' in solids? J Phys C: Solid State Phys 6, L422 (1973).
13. S. Ljunggren. A simple graphical representation of Fourier-based imaging methods. J Magn Res 54, 338 (1983).
14. D. B. Twieg. The k-trajectory formulation of the NMR imaging process with applications in analysis and synthesis of imaging methods. Med Phys 10, 610 (1983).
15. W. A. Edelstein, J. M. S. Hutchison, G. Johnson, and T. Redpath. Spin warp NMR imaging and applications to human whole-body imaging. Phys Med Biol 25, 751 (1980).

16. A. Kumar, D. Welti, and R. Ernst. NMR Fourier zeugmatography. J Magn Res 18, 69 (1975).

17. P. C. Lauterbur. Image formation by induced local interactions: examples employing nuclear magnetic resonance. Nature 242, 190 (1973).

18. C. M. Lai and P. C. Lauterbur. True three-dimensional image reconstruction by nuclear magnetic resonance zeugmatography. Phys Med Biol 26, 851 (1981).

19. I. R. Young, D. R. Bailes, M. Burl, A. G. Collins, D. T. Smith, M. J. McDonnel, J. S. Orr, M. L. Banks, G. M. Bydder, R. H. Greespan, and R. E. Steiner. Initial clinical evaluation of a whole-body nuclear magnetic resonance (NMR) tomograph. J Comput assist Tomogr 6, 1 (1982).

20. A. Macovski. Volumetric NMR imaging with time-varying gradients. Magn Res Medicine 2, 29 (1985).

21. C. Ahn, J. Kim, and Z. Cho. High-speed spiral-scan echo planar NMR imaging --I. IEE Trans Med Imaging MI-5, 2 (1986).

22. C. H. Meyer, B. Hu, D. G. Nishimura, and A. Macovski. Fast spiral coronal artery imaging. Magn Reson Med 28, 202 (1992).

23. A. Haase. Snapshot FLASH MRI. Applications to T1, T2 and chemical shift imaging. Magn Res Medicine 13, 77 (1990).

24. J. Frahm, K. D. Merboldt, H. Bruhn, M. L. Gyngell, et al. 0.3 second FLASH MRI of the human heart. Magn Res Medicine 13, 150 (1990).

25. P. Brunner and R. R. Ernst. Sensitivity and performance time in NMR imaging. J Magn Reson 33, 83 (1979).

26. L. E. Crooks, C. M. Mills, P. L. Davis, M. Brant-Zawadski, and J. Hoenninger. Visualization of cerebral and vascular abnormalities by NMR imaging. The effects of imaging parameters on contrast. Radiol 144, 843 (1982).

27. J. R. MacFall, M. Pelc, and R. M. Vavrek. Correction of spatially dependent phase shifts in partial Fourier imaging. Magn Res Imaging 6, 143 (1988).

28. P. Margosian, F. Schmitt, and D. Purdy. Faster MR imaging: imaging with half the data. Health Care Instrum 1, 195 (1986).

29. D. Feinberg, J. Hale, J. Watts, and et. al. Halving MR imaging time by conjugation: Demonstration at 3.5 kG. Radiol 161, 527 (1986).

30. R. R. Ernst and W. A. Anderson. Application of Fourier transform spectroscopy to magnetic resonance. Rev Sci Inst 37, 93 (1966).

31. J. Ma, F. Wehrli, and H. Song. Fast 3D large-angle spin-echo imaging (3D FLASE). Magn Reson Medicine 35, 903 (1996).

32. H. K. Song, F. W. Wehrli, and J. Ma. In vivo MR microscopy of the human skin. Magn

Reson Medicine In press, (1996).

33. T. K. F. Foo, F. G. Shellock, C. E. Hayes, J. F. Schenck, and B. E. Slayman. High-resolution MR imaging of the wrist and eye with short TR, short TE and partial-echo acquisition. Radiol 183, 277 (1992).

34. A. E. H. Bampton, S. J. Riederer, and H. W. Korin. Centric phase-encoding order in three-dimensional MP-RAGE. J Magn Res Imaging 2, 227 (1992).

35. J. P. 3. Mugler and R. Brookeman J. Rapid three-dimensional T1-weighted MR imaging with the MP-RAGE sequence. J Magn Reson Imaging 1, 561 (1991).

36. J. P. 3. Mugler, T. A. Spraggins, and J. R. Brookeman. T2-weighted three-dimensional MP-RAGE MR imaging. J Magn Reson Imaging 1, 731 (1991).

37. G. Nayler, D. N. Firmin, and D. B. Longmore. Blood flow imaging by cine magnetic resonance. J Comput Assist Tomogr 10, 715 (1986).

38. G. H. Glover and N. J Pelc. Eds., A rapid-gated cine MRI technique (Raven Press, New York, 1988).

39. D. J. Atkinson and R. R. Edelman. Cineangiography of the heart in a single breath hold with a segmented turbo FLASH sequence. Radiol 178, 357 (1991).

40. T. K. Foo, M. A. Bernstein, A. M. Aisen, R. J. Hernandez, B. D. Collick, and T. Bernstein. Improved ejection fraction and flow velocity estimates with use of view sharing and uniform repetition time excitation with fast cardiac techniques. Radiol 195, 471 (1995).

41. P. Mansfield and I. L. Pykett. Biological and Medical Imaging by NMR. J Magn Res 29, 355 (1978).

42. B. Chapman, R. Turner, R. Ordidge, M. Doyle, Mr. Cawley, R. Coxon, P. Glover, and P. Mansfield. Real-time movie imaging from a single cardiac cycle by NMR. Magn Reson Med 5, 246 (1987).

43. A. M. Houseman, M. K. Stehling, B. Chapman, et. al. Improvements in snapshot NMR imaging. Br J Radiol 61, 822 (1988).

44. M. S. Cohen and R. M. Weisskoff. Ultra-fast imaging. Magn Res Imaging 9, 1 (1991).

45. G. McKinnon. Ultrafast interleaved gradient echo planar imaging on a standard scanner. Magn Reson Med 30, 609 (1993).

46. K. Butts, S. J. Riederer, R. L. Ehman, R. M. Thompson, and C. R. Jack. Interleaved echo planar imaging on a standard MRI system. Magn Reson Med 31, 67 (1994).

47. J. Hennig, A. Nauerth, and H. Friedburg. RARE imaging: A fast imaging method for clinical MR. Magn Res Medicine 3, 823 (1986).

48. P. S. Melki, R. V. Mulkern, L. P. Panych, and F. A. Jolesz. Comparing the FAISE method with conventional dual-echo sequences. Magn Res Imaging 1, 319 (991).

49. P. S. Melki, F. A. Jolesz, and R. V. Mulkern. Partial RF echoplanar imaging with the FAISE method: I. Experimental and theoretical assessment of artifact. Magn Res Medicine 26, 328 (1992).

50. P. S. Melki, P. S. Melki, F. A. Jolesz, and R. V. Mulkern. Partial RF echoplanar imaging with the FAISE method: II. Contrast equivalence with spin-echo sequence. Magn Res Medicine 26, 342 (1992).

51. C. Yuan, P. Schmiedl U, E. Weinberger, R. Krueck W, and D. Rand S. Three-dimensional fast spin-echo imaging: pulse sequence and in vivo imaging evaluation. J Magn Reson Imaging 3. 894 (1993).

52. D. A. Feinberg and K. Oshio. GRASE (Gradient-and Spin-Echo) MR imaging: a new fast clinical imaging technique. Radiol 181, 597 (1991).

53. J. Hennig. Multi-echo imaging sequences with low refocusing flip angles. J Magn Reson 78, 397 (1988).

54. D. D. Alsop. The sensitivity of low flip angle RARE imaging. Magn Reson Medicine in press, 1 (1996).

55. P. Mansfield and P. R. Harvey. Limits to neural stimulation in echo-planar imaging. Magn Reson Medicine 29, 746 (1993).